Theoretical and Experimental Investigation of a 2 × 2 MIMO OFDM Radio-Over-Fiber System at 60-GHz With I/Q Imbalance Compensation

Chun-Hung Ho, *Student Member, IEEE*, Chun-Ting Lin, *Member, IEEE*, Tsung-Hung Lu, Hou-Tzu Huang, Boris (Po-Tsung) Shih, Chia-Chien Wei, and Anthony Ng'oma, *Member, IEEE*

***Abstract*—This paper investigates the efficacy of two methods for compensating I/Q imbalance, which causes serious performance problems in wideband (6.98-GHz spectrum) millimeter-wave systems employing MIMO signal transmission. A 60-GHz orthogonal frequency division multiplexing (OFDM) RoF system employing 2 × 2 MIMO technology is implemented using a commonly used training symbol arrangement and a proposed method. We experimentally demonstrate that the proposed training symbol arrangement performed significantly better than the commonly used approach. By combining the proposed training symbol arrangement with LMS I/Q compensation and bit-loading, we achieve an extremely high wireless data rate transmission of 75.211 Gb/s over both 50 km of standard single-mode fiber and 3.5-m wireless distance. The optical power penalty after 50-km fiber transmission was only ~1 dB.**

***Index Terms*—I/Q imbalance, MIMO, optical fiber communication, wireless communication.**

I. Introduction

TO realize multi-Gb/s transmission for broadband wireless applications, 60-GHz technology has been highlighted as a potential candidate within the license-free band [1], [2]. However, the signal coverage of a single 60-GHz antenna unit is extremely limited compared with conventional wireless technologies (e.g., cellular and WiFi) due to the high wireless transmission loss and attenuations through walls. Radio-over-Fiber (RoF) technologies, which deliver radio-frequency over low loss optical fibers, have been extensively investigated to extend the 60-GHz wireless signal coverage. To generate and distribute high capacity 60-GHz signals efficiently, frequency-multiplication modulation techniques with advanced modulation formats are utilized. Moreover, to compensate for the channel impairments and increase the spectra-efficiency, digital signal processing (DSP) techniques, such as bit-loading and phase noise compensation algorithms, have been implemented with the 60-GHz RoF systems [3]–[9].

I/Q imbalance, which is one of the channel impairments, comes from the imperfect amplitude and phase mismatch between the in-phase (I) and quadrature-phase (Q) channels during the signal I/Q modulation. For an orthogonal frequency division multiplexing (OFDM) signal, the subcarriers are distorted by the mirror-images of symmetrical subcarriers and significantly impact the system performance due to I/Q imbalance. Conventional time-domain compensation algorithms are difficult to overcome I/Q imbalance [10]–[13]. Therefore, frequency-domain compensation algorithms, such as decision-aided joint method and pilot-assisted method are proposed to overcome this channel impairment efficiently [14], [15]. However, the decision-aided joint method requires more complex algorithms to compensate for the I/Q mismatch and phase noise at the same time, and the signal distortions will be enlarged while the decision errors happen over long distance fiber transmission. For the pilot-assisted method, it requires to sacrifice signal bandwidth for I/Q imbalance estimation. Therefore, recursive least squares (RLS) and least mean squares (LMS) algorithms are proposed to compensate for the I/Q imbalance without complex algorithms and decreasing throughput, and 40 Gb/s wireless transmission can be experimentally achieved in a 60-GHz single-input single-output (SISO) system [16].

MIMO technology has emerged as a critical technology for increasing the wireless channel capacity or reliability of modern wireless communication systems [17], [18]. More recently, the technology has been investigated for use in fiber-wireless systems [19]–[21]. However, the performance of wideband 60-GHz systems employing MIMO is severely impacted by I/Q imbalance, which is caused firstly by the I/Q modulator followed by mixing during MIMO signal transmission. The presence of mixed I/Q imbalance in the transmitted MIMO signals makes it difficult to accurately estimate the MIMO channel resulting in poor data recovery. In this paper, we theoretically and experimentally investigate the efficacy of two kinds of training symbol arrangements for compensating I/Q imbalance impairments in wideband 60-GHz MIMO RoF systems. We demonstrate experimentally that the proposed training symbol arrangement performed significantly better than the commonly used approach, resulting in extremely high wireless data transmission of >75 Gb/s over both 50 km of standard single-mode fiber and 3.5 m wireless distance.

Manuscript received January 15, 2014; revised April 4, 2014; accepted February 20, 2014. Date of publication May 19, 2014; date of current version September 1, 2014.

C.-H. Ho, C.-T. Lin, T.-H. Lu, and H.-T. Huang are with the Institute of Photonic System, National Chiao-Tung University, Tainan 711, Taiwan (e-mail: cunhonho@gmail.com; jinting@mail.nctu.edu.tw; tsunghunglu@gmail.com; whang.kurt@gmail.com).

B. Shih is with Corning Research Center Taiwan, Corning Inc., Hsinchu 310, Taiwan (e-mail: ShihPT@corning.com).

C.-C. Wei is with the Department of Photonics, National Sun Yat-Sen University, Kaohsiung 804, Taiwan (e-mail: ccwei@mail.nsysu.edu.tw).

A. Ng'oma is with Corning Inc., Corning, New York, NY 14831 USA (e-mail: ngomaa@corning.com).

Color versions of one or more of the figures in this paper are available online at http://ieeexplore.ieee.org.

Digital Object Identifier 10.1109/JLT.2014.2325816

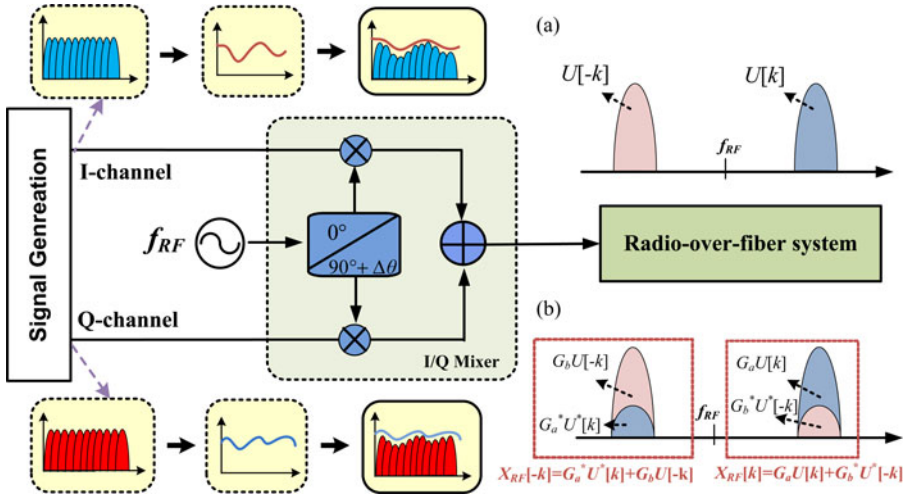

Fig. 1. Conceptual diagram of an I/Q up-conversion system. (f_{RF} : carrier frequency) (a) OFDM subcarrier signal without I/Q imbalance. (b) OFDM subcarrier signal with I/Q imbalance.

The rest of this paper is organized as the following. In Section II, theoretical analysis of I/Q imbalance in a 2 × 2 MIMO wireless channel is discussed. In Section III, the principles of two kinds of TSs and I/Q imbalance compensation are derived. Experimental setup, results, and comparison are described and commented in Section IV and Section V, respectively. Finally, conclusions are given in Section VI.

II. I/Q Imbalance in MIMO OFDM System

To generate 60-GHz signal in a RoF system, either electrical or optical up-conversion [4], [16], [22] at transmitter is required. However, due to the 7-GHz wide bandwidth at 60-GHz, I/Q imbalance interference cannot be prevented in both electrical and optical up-conversion. Fig. 1 illustrates the conceptual diagram of an OFDM up-conversion with an electrical I/Q mixer. With the mismatches of phase and amplitude between OFDM I and Q channels, the *k*th OFDM subcarrier ($X[k]$) will have I/Q imbalance interference from the mirror-image –*k*th OFDM subcarriers ($X[-k]$) as shown in the insets (a) and (b) of Fig. 1, where $k = -N/2$ to $N/2$, and N is the number of OFDM subcarriers. Therefore, the corresponding OFDM subcarriers with I/Q imbalance can be mathematically expressed as [23]

$$X[k] = G_a U[k] + G_b^* U^*[-k]. \tag{1}$$

$$X[-k] = G_b U[-k] + G_a^* U^*[k] \tag{2}$$

$$G_a = \frac{1+\Delta\xi e^{j\Delta\theta}}{2}, \quad G_b = \frac{1-\Delta\xi e^{-j\Delta\theta}}{2} \tag{3}$$

where $(.)^*$ denotes conjugate operation. $U[k]$ and $U[-k]$ represent the *k*th and the –*k*th OFDM subcarriers without I/Q imbalance. G_a and G_b are I/Q imbalance coefficients, which are the function of amplitude imbalance ratio ($\Delta\xi$) and phase deviation range ($\Delta\theta$), where $0 \le \Delta\xi \le 1$ and $0 \le \Delta\theta \le \pi/2$. In a SISO system, I/Q imbalance compensation based on LMS and RLS algorithm have been proposed to adaptively correct the imbalance coefficients in equations (1) and (2) [16], [24].

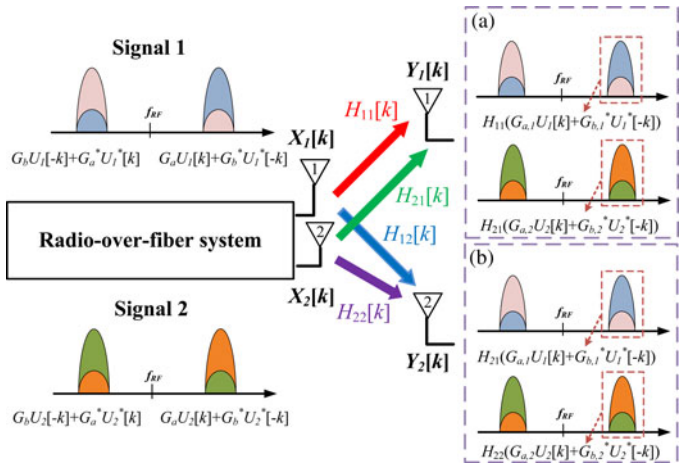

Fig. 2. 2 × 2 MIMO wireless channel mixing with the impact of I/Q imbalance. (a) MIMO signal 1. (b) MIMO signal 2.

Fig. 2 illustrates the impact of I/Q imbalance over a 2 × 2 MIMO wireless transmission. Before wireless transmission, each subcarrier is only influenced from mirror-image interference at each transmitter. After wireless transmission, two streams of MIMO signals suffer additional cross-interferences from the other transmitter as shown in the insets (a) and (b) of Fig. 2. Two streams of *k*th OFDM subcarriers can be expressed as

$$\begin{bmatrix} Y_1[k] \\ Y_2[k] \end{bmatrix} = \mathbf{H} \begin{bmatrix} X_1[k] \\ X_2[k] \end{bmatrix} + \mathbf{W} \tag{4}$$

$$\mathbf{H} = \begin{bmatrix} H_{11}[k] & H_{21}[k] \\ H_{12}[k] & H_{22}[k] \end{bmatrix} \tag{5}$$

where $X_i[k]$, $Y_j[k]$, and $\mathbf{W}$ represent transmitted OFDM signals, received OFDM signals, and additive Gaussian noise vector, respectively. $\mathbf{H}$ is the 2 × 2 MIMO wireless channel matrix composed of four channel coefficients, and $H_{ij}[k]$ represents

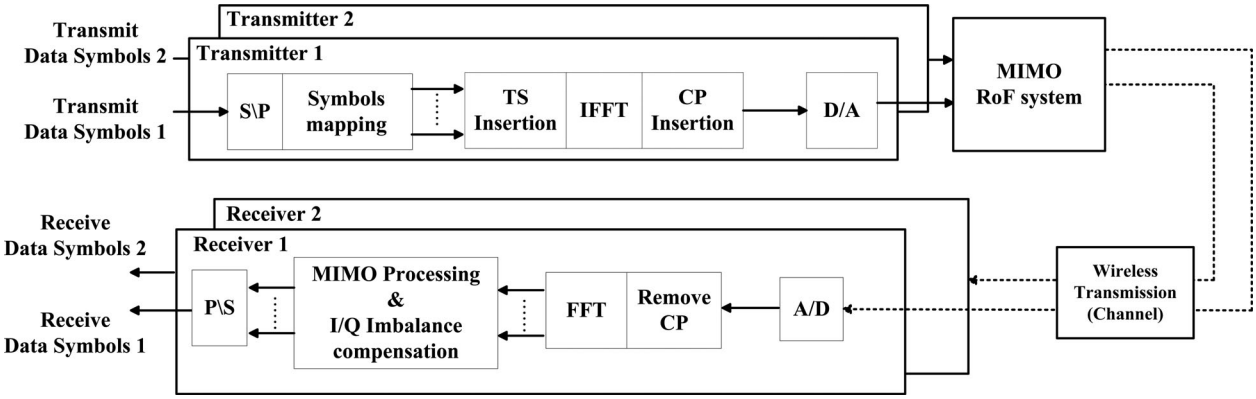

Fig. 3. Block diagrams of 2 × 2 MIMO OFDM RoF system with I/Q imbalance compensation. S\P: Series to parallel; P\S: Parallel to series; (I)FFT: (Inverse) Fast Fourier transform; D/A: Digital to analogue; A/D: Analogue to digital.

channel coefficients from the *i*th transmitted antenna to the *j*th received antenna, where $i, j = 1, 2$. With I/Q imbalance at wireless transmitters, equation (4) can be modified as

$$\begin{bmatrix} Y_1[k] \\ Y_2[k] \end{bmatrix} = \begin{bmatrix} H_{11}[k] & H_{21}[k] \\ H_{12}[k] & H_{22}[k] \end{bmatrix} \begin{bmatrix} G_{a,1}U_1[k] + G_{b,1}^* U_1^*[-k] \\ G_{a,2}U_2[k] + G_{b,2}^* U_2^*[-k] \end{bmatrix} + \mathbf{W} \quad (6)$$

$$= \begin{bmatrix} H_{11}[k] & H_{21}[k] \\ H_{12}[k] & H_{22}[k] \end{bmatrix} \begin{bmatrix} G_{a,1} & 0 \\ 0 & G_{a,2} \end{bmatrix} \begin{bmatrix} U_1[k] \\ U_2[k] \end{bmatrix} + \begin{bmatrix} H_{11}[k] & H_{21}[k] \\ H_{12}[k] & H_{22}[k] \end{bmatrix} \begin{bmatrix} G_{b,1}^* & 0 \\ 0 & G_{b,2}^* \end{bmatrix} \begin{bmatrix} U_1^*[-k] \\ U_2^*[-k] \end{bmatrix} + \mathbf{W} \quad (7)$$

$$\Rightarrow \mathbf{Y} = \mathbf{H}\mathbf{G_a}\mathbf{U} + \mathbf{H}\mathbf{G_b}\mathbf{U}' + \mathbf{W}. \quad (8)$$

where $U = [U_1[k]\, U_2[k]]^{\mathrm{T}}$ is the signal vector without I/Q imbalance influence. G_a and G_b are the matrices of I/Q imbalance coefficients, i.e. $G_{a,i}$ and $G_{b,i}$, and can be defined as

$$G_{a,1} = \frac{1 + \Delta\xi_1 e^{j\Delta\theta_1}}{2}, \quad G_{b,1} = \frac{1 - \Delta\xi_1 e^{-j\Delta\theta_1}}{2}$$
$$G_{a,2} = \frac{1 + \Delta\xi_2 e^{j\Delta\theta_2}}{2}, \quad G_{b,2} = \frac{1 - \Delta\xi_2 e^{-j\Delta\theta_2}}{2}. \quad (9)$$

III. Training Symbol Design and I/Q Imbalance Compensation

Fig. 3 shows the block diagrams of the utilized 2 × 2 MIMO communication system. The OFDM signal generation includes serial to parallel (S/P) conversion, symbols mapping, insertion of TSs, inverse fast Fourier transform (IFFT), insertion of cyclic prefix (CP) and digital to analog conversion (D/A). After transmitting over the RoF system and the wireless 2 × 2 MIMO channels, the signal demodulation involves analog to digital conversion (A/D), CP removal, fast Fourier transform (FFT), MIMO processing, and I/Q imbalance compensation. In order to demodulate MIMO signals, TSs are utilized to estimate equalization parameters and the channel coefficients for data recovery [25].

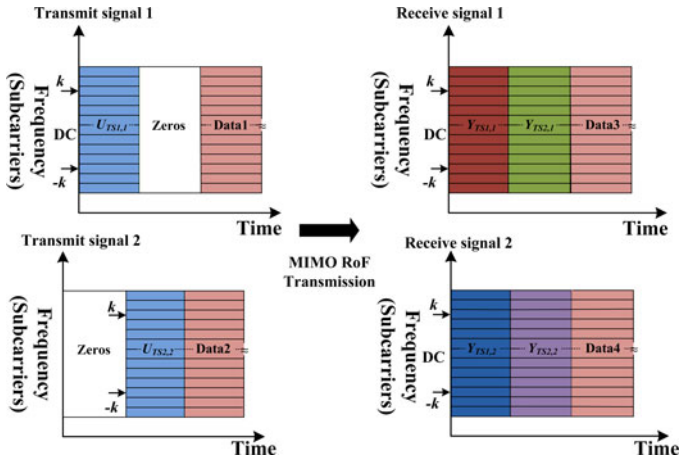

Fig. 4. Training symbols (TS I) arrangement with interleaved on-off order in the time domain.

A. First Kind of Training Symbol

To effectively avoiding the MIMO interference during channel coefficients estimation, TS I, which is commonly used, is implemented by interleaved ON–OFF orders in the time domain with equal length as shown in Fig. 4. To estimate the channel coefficients, the equation (8) can be modified as

$$\mathbf{H}\mathbf{G_a} = \mathbf{U}^{-1}\mathbf{Y} + \mathbf{U}^{-1}\mathbf{H}\mathbf{G_b}\mathbf{U}' + \mathbf{U}^{-1}\mathbf{W}. \quad (10)$$

The interference term from the mirror-image subcarriers in the equation (10), i.e. $\mathbf{U}^{-1}\mathbf{H}\mathbf{G_b}\mathbf{U}'$, can be ignored due to zero-mean condition of that if the number of TS I is large enough.

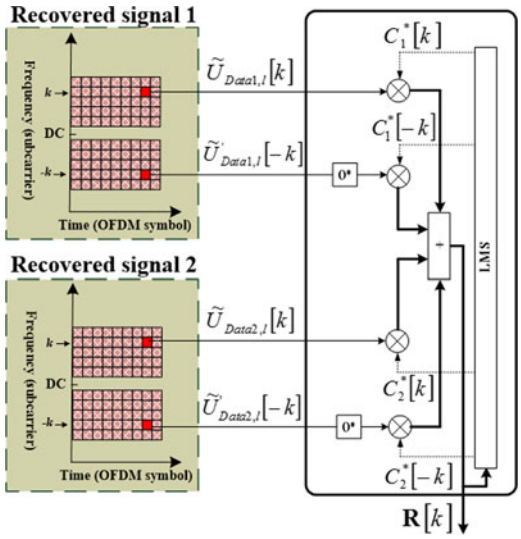

Fig. 5. Concept of adaptive IQ imbalance compensation based on LMS algorithm in frequency-domain for 2 × 2 MIMO signals.

Then, the channel matrix can be estimated and expressed as

$$\tilde{\mathbf{K}}_{\mathbf{a}} = \mathbf{H}\mathbf{G}_{\mathbf{a}} = \begin{bmatrix} Y_{TS1,1}/U_{TS1,1}[k] & Y_{TS1,2}/U_{TS2,2}[k] \\ Y_{TS2,1}/U_{TS1,1}[k] & Y_{TS2,2}/U_{TS2,2}[k] \end{bmatrix} \tag{11}$$

where $\tilde{\mathbf{K}}_{\mathbf{a}}$ is the estimated channel matrix. By using Zero-forcing algorithm [26], the recovered MIMO kth OFDM subcarrier signal vectors can be expressed as

$$\tilde{\mathbf{U}}_{\mathbf{Data}} = \tilde{\mathbf{K}}_{\mathbf{a}}^{-1}\mathbf{Y}_{\mathbf{Data}} = \mathbf{U}_{\mathbf{Data}} + \mathbf{G}_{\mathbf{a}}^{-1}\mathbf{G}_{\mathbf{b}}\mathbf{U}'_{\mathbf{Data}} \tag{12}$$

$$= \mathbf{U}_{\mathbf{Data}} - \begin{bmatrix} \frac{G^*_{b,1}}{G_{a,1}} & 0 \\ 0 & \frac{G^*_{b,2}}{G_{a,2}} \end{bmatrix} \mathbf{U}'_{\mathbf{Data}} \tag{13}$$

where $\tilde{\mathbf{U}}_{\mathbf{Data}} = \left[\tilde{U}_{\mathrm{Data1}}[k]\, \tilde{U}_{\mathrm{Data2}}[k]\right]^{\mathrm{T}}$ is the recovered MIMO OFDM signals vector. Since the interference terms from the mirror-image subcarriers will cause signal degradation, I/Q imbalance compensation based on LMS algorithm is implemented to adaptively correct the signals. Fig. 5 describes the concept of the I/Q imbalance compensation in frequency domain. After adaptive correction, the output signal can be expressed as

$$\mathbf{R}_l = (\mathbf{C}_l)^* \cdot \tilde{\mathbf{U}}''_l. \tag{14}$$

where $\mathbf{R}_l$, $\mathbf{C}_l$ represent the corrective signal vectors and I/Q imbalance corrective coefficient vectors represent input signal vectors $\tilde{\mathbf{U}}_l = \left[\tilde{\mathbf{U}}_{\mathrm{Data1},l}[k]\, \tilde{\mathbf{U}}_{\mathrm{Data1},l}[-k]\, \tilde{\mathbf{U}}_{\mathrm{Data2},l}[k]\, \tilde{\mathbf{U}}_{\mathrm{Data2},l}[-k]\right]^{\mathrm{T}}$ on lth OFDM symbol. The LMS algorithm is used to update imbalance corrective coefficient vectors by minimizing mean square error criterion:

$$\mathbf{E}_l = \mathbf{S}_l - \mathbf{R}_l \tag{15}$$

$$\mathbf{C}_{l+1} = \mathbf{C}_l + u \cdot (\mathbf{E}_l)^* \cdot \mathbf{R}_l \tag{16}$$

where $\mathbf{E}_l$, $\mathbf{S}_l$, and u are error vectors, decision signal vectors and converge coefficient.

B. Second Kind of Training Symbol

Fig. 6 shows schematic diagram of TS II with ON–OFF order both in time-domain and frequency-domain. TS II includes four equal time slots. In each time slot, only half of OFDM subcarriers in one of the two transmitters are modulated with non-zero signals, where $k = 1$ to $N/2$, and N is the number of OFDM subcarrier. Hence, the received TS II can be generally expressed as

$$\begin{bmatrix} Y_1[k] \\ Y_2[k] \\ Y_1^*[-k] \\ Y_2^*[-k] \end{bmatrix} = \mathbf{H}\mathbf{U} + \mathbf{W}$$

$$= \begin{bmatrix} H_{11} & H_{12} & H_{13} & H_{14} \\ H_{21} & H_{22} & H_{23} & H_{24} \\ H_{31} & H_{32} & H_{33} & H_{34} \\ H_{41} & H_{42} & H_{43} & H_{44} \end{bmatrix} \begin{bmatrix} U_1[k] \\ U_1^*[-k] \\ U_2[k] \\ U_2^*[-k] \end{bmatrix} + \mathbf{W}. \tag{17}$$

where $\mathbf{U}$ is the signal vector without I/Q imbalance. $\mathbf{H}$ is a 4×4 channel matrix which is composed of channel coefficients, and can be estimated from TS II as the following: (See eq.18 in bottom of this page).

Then, the MIMO signal could be recovered:

$$\begin{bmatrix} \tilde{U}_{\mathrm{Data1}}[k] \\ \tilde{U}^*_{\mathrm{Data1}}[-k] \\ \tilde{U}_{\mathrm{Data2}}[k] \\ \tilde{U}^*_{\mathrm{Data2}}[-k] \end{bmatrix} = \mathbf{H}^{-1} \begin{bmatrix} Y_{\mathrm{Data1}}[k] \\ Y^*_{\mathrm{Data1}}[-k] \\ Y_{\mathrm{Data2}}[k] \\ Y^*_{\mathrm{Data2}}[-k] \end{bmatrix}. \tag{19}$$

IV. Experimental Setup

Fig. 7 schematically shows the experimental setup of a RoF system with 2 × 2 MIMO wireless transmission at 60-GHz. The optical transmitter is simply composed of a 40-GHz single-electrode MZM and an electrical I/Q mixer. The signals had

$$\mathbf{H} = \begin{bmatrix} Y_{TS1,1}[k]/U_{TS1,1}[k] & Y_{TS2,1}[k]/U^*_{TS2,1}[-k] & Y_{TS3,1}[k]/U_{TS3,2}[k] & Y_{TS4,1}[k]/U^*_{TS4,2}[-k] \\ Y_{TS1,1}[-k]/U_{TS1,1}[k] & Y_{TS2,1}[-k]/U^*_{TS2,1}[-k] & Y_{TS3,1}[-k]/U_{TS3,2}[k] & Y_{TS4,1}[-k]/U^*_{TS4,2}[-k] \\ Y_{TS1,2}[k]/U_{TS1,1}[k] & Y_{TS2,2}[k]/U^*_{TS2,1}[-k] & Y_{TS3,2}[k]/U_{TS3,2}[k] & Y_{TS4,2}[k]/U^*_{TS4,2}[-k] \\ Y_{TS1,2}[-k]/U_{TS1,1}[k] & Y_{TS2,2}[-k]/U^*_{TS2,1}[-k] & Y_{TS3,2}[-k]/U_{TS3,2}[k] & Y_{TS4,2}[-k]/U^*_{TS4,2}[-k] \end{bmatrix}. \tag{18}$$

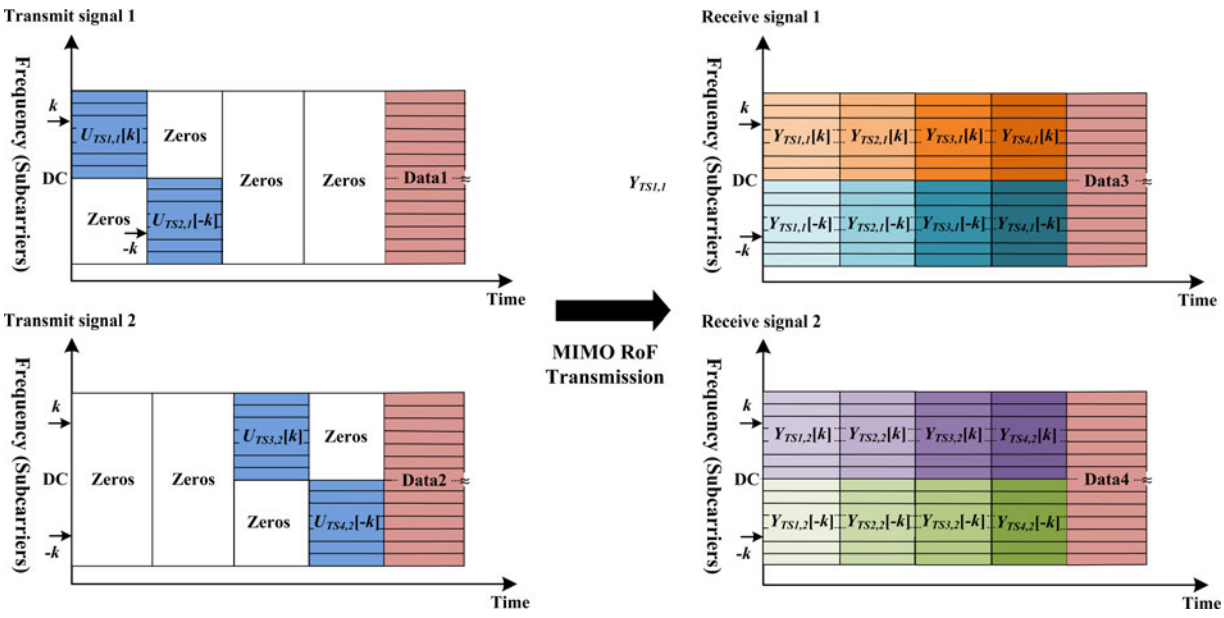

Fig. 6. Training symbols (TS II) arrangement with interleaved ON–OFF order both in frequency domain and time domain.

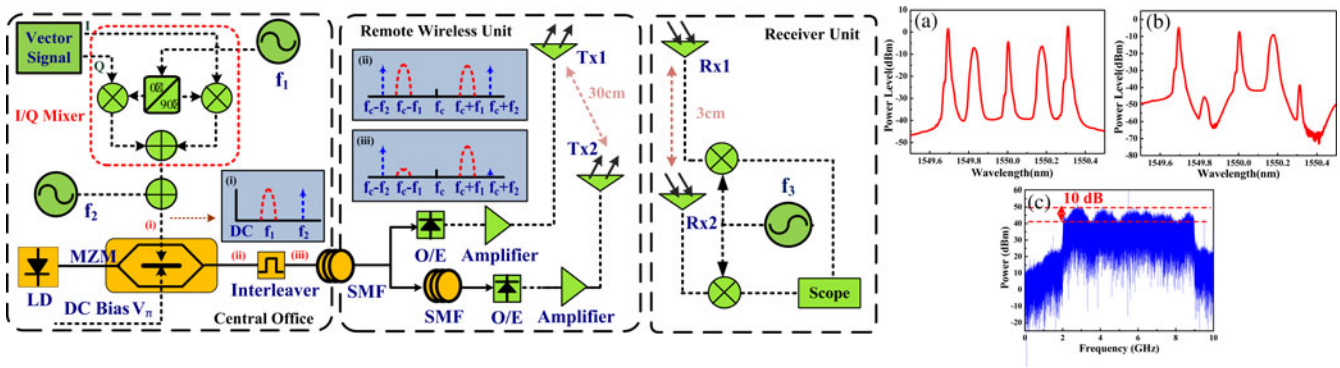

Fig. 7. Experimental setup for 2 × 2 MIMO OFDM RoF system ($f_1 = 21.5$ GHz, $f_2 = 39$ GHz, $f_3 = 55$ GHz) and optical spectrum. (a) After MZM. (b) After optical interleaver. (c) Electrical spectrum after down-conversion.

IFFT and FFT size of 512 points and 298 subcarriers with different modulation formats (i.e. 16-QAM and 32-QAM) among 6.98 GHz bandwidth. The CP is fixed at 16 points over IFFT/FFT size. TSs were inserted in front of the data streams. The length of TS is continued for 16 and 32 OFDM symbols time for TS I and TS II, respectively. I and Q channels of the OFDM signals were generated by an arbitrary waveform generator with sampling rate of 12-GSa/s. Both I and Q signals were sent into an electrical I/Q mixer with 9-GHz IF bandwidth and up-converted to 21.5 GHz (f_1). The 21.5-GHz OFDM signal was subsequently combined with the 39-GHz (f_2) sinusoidal signal to drive the optical modulator, as shown in inset (i) of Fig. 7. The bias voltage of the MZM was set at the null point to achieve the optical double-sideband with carrier suppression scheme as shown in the inset (ii) of Fig. 7 and the generated optical spectrum is shown in Fig. 7(a). In order to overcome the power fading induced by fiber transmission, a 33/66-GHz optical interleaver was implemented as an optical filter to remove un-desired sidebands as shown in inset (iii) of Fig. 7 and the optical spectrum in Fig. 7(b). To imitate the MIMO signal generation, the optical signal was split by a 50:50 optical coupler after the fiber transmission, and one of the optical signals was delayed by an additional 2-km single-mode fiber to decorrelate the two signals. After photodiode detection, two 60.5-GHz electrical signals were generated and fed into two standard gain horn antennas with 23 dBi gain and 30 cm apart to each other. After 3.5-m wireless transmission, the two streams of MIMO signals were received by the two antennas with 3 cm apart and separately down-converted to 5.5-GHz as shown with a 55-GHz (f_3) sinusoidal signal in Fig 7. The electrical spectrum of one of the down-converted MIMO signal is shown in Fig. 7(c). These down-converted signals were captured separately by a scope with 80-GSa/s sampling rate and 16-GHz analog bandwidth. Consequently, the received signals were demodulated using off-line DSP programs. Signal synchronization, FFT, channel estimation with one-tap equalizer, MIMO processing and LMS I/Q imbalance

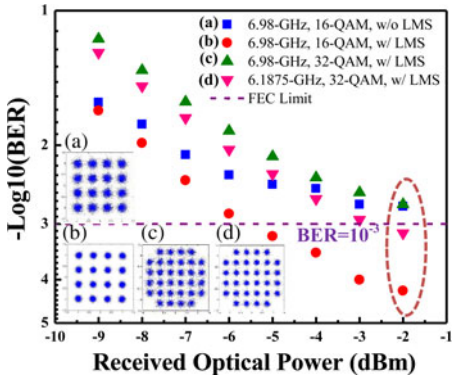

Fig. 8. Combined BER versus received optical power curves of 6.98-GHz 16-QAM, 32-QAM, and 6.1875-GHz 32-QAM 2 × 2 MIMO OFDM signals without and with LMS I/Q imbalance compensation at BTB with 3.5-m wireless transmission, and constellation diagrams of (a) 6.98-GHz, 16QAM without LMS I/Q compensation algorithm. (b) 6.98-GHz, 16QAM with LMS I/Q compensation algorithm. (c) 6.98-GHz, 32QAM without LMS I/Q compensation algorithm. (d) 6.1875-GHz, 32QAM with LMS I/Q compensation algorithm.

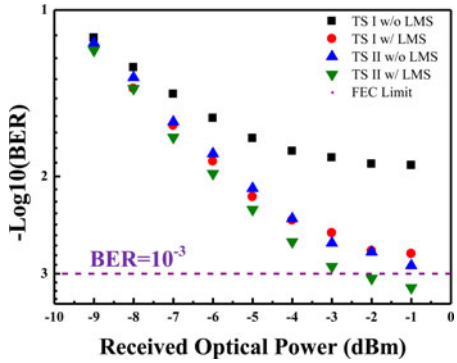

Fig. 9. Combined BER versus received optical power curves of 6.98-GHz 32-QAM 2 × 2 MIMO OFDM signals with two kinds of TS at BTB with 3.5-m wireless transmission.

compensation were performed in series in the off-line DSP programs. Since the impact of phase rotation induced from carrier frequency offset can be easily compensated by the limited TSs in direct detection system with stable channel condition, the overhead of TSs can be ignored along with long data streams. Following discussions about line data rate are without removing the overhead of cp (3.125%). In order to make continuous investigation, the forward error correction (FEC) BER requirement consists with the same threshold (1×10^{-3}) in the previous work [4], [6], [16], [27].

V. Experimental Results and Discussions

In the proposed system, I/Q imbalance takes place mainly at the transmitter side and dominated by the I/Q electrical mixer. By using TS I, Fig. 8 shows the combined average bit error rate (BER) of the two received signals versus the received optical power between −2 and −9 dBm for the back-to-back (BTB) case. Without any I/Q imbalance compensation algorithm, the 16-QAM OFDM signal with 6.98-GHz bandwidth could not meet the FEC BER requirement. To reduce the impact of I/Q imbalance, compensation based on the LMS algorithm was implemented resulting in significant improvement in the BER performance, and the achievement of 55.875 Gb/s data rate at the BER FEC threshold and −5.5 dBm received optical power. To increase the data rate, the 32-QAM OFDM signal was also transmitted with 6.98-GHz bandwidth. However, FEC BER requirement could not be reached even with LMS I/Q imbalance compensation—meaning the system could not achieve the target line data rate of 69.843 Gb/s. Therefore, the signal bandwidth was decreased to 6.1875-GHz to overcome distortion limitations encountered with the wider 6.98-GHz spectrum. This allowed the system with 32-QAM modulation to meet the minimum FEC BER requirement with higher line data rate of 61.875 Gb/s at the received optical power of −3 dBm. Insets (a)–(d) in Fig. 8 show the clear constellation diagrams of 16-QAM and 32-QAM signals at the optical power of −2 dBm.

To determine the performance of the proposed training symbol arrangement (TS II) the transmission experiments were repeated, but this time with the new training symbol arrangement instead of the commonly used one. Fig. 9 shows the BER performance comparison between the two of TS arrangements with 6.98-GHz 32-QAM OFDM signals over 3.5-m wireless transmission. The results show that the proposed training symbol arrangement performs significantly better than the first one. In this case, the 32-QAM OFDM MIMO signals with TS II, but without LMS I/Q imbalance compensation was able to provide similar system performance to the system using TS I with LMS I/Q imbalance compensation. This is attributed to the fact that TS II arrangement does a better job of minimizing the impact of the I/Q imbalance during the recovery of MIMO data and hence accurately estimating the MIMO channel. This result is consistent with the theoretical prediction described in Section III. However, using the TS II alone, the FEC BER requirement cannot be achieved even with −1 dBm received optical power due to the impact of residual I/Q imbalance. As shown in Fig. 9, using TS II with LMS I/Q imbalance compensation, FEC BER requirement could be achieved with 6.98-GHz 32-QAM OFDM MIMO signals. The achievable line data rate was 69.843 Gb/s with received optical power of −2.5 dBm. Although higher overhead (double time slots) is required with TS II, better system performance could be achieved compared with TS I.

To further understand the performance limitations of the proposed MIMO OFDM system with I/Q imbalance, TS I and TS II with fiber transmission distance from BTB to 50-km were investigated. Fig. 10 shows the BER versus received optical power curves of 6.98-GHz 16-QAM and 6.1875-GHz 32-QAM OFDM signals using TS I with LMS I/Q imbalance compensation over 3.5-m wireless transmission. With 16-QAM modulation format, it could be observed that there was no power penalty between BTB and 25-km transmission, and the power penalty was less than 0.5 dB between BTB and 50-km transmission. With 32-QAM modulation format, however, the power penalties were about 0.5 dB between BTB and 25-km transmission and 2 dB between BTB and 50-km transmission. FEC BER requirement could be achieved with both formats. Insets

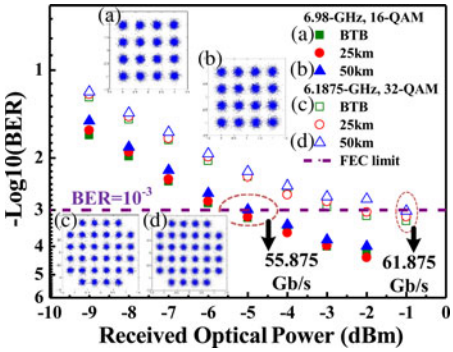

Fig. 10. Combined BER versus received optical power curves of 6.98-GHz 16-QAM (line data rate: 55.875-Gb/s) and 6.1875-GHz 32-QAM (line data rate: 61.875-Gb/s) 2 × 2 MIMO OFDM signals over fiber transmission from BTB to 50-km and 3.5-m wireless transmissions with TS I and LMS I/Q imbalance compensation. (a) and (b) Constellation diagrams of 16-QAM at −5 dBm received optical power from BTB to 50-km fiber transmission (c) and (d) 32-QAM at –1 dBm received optical power from BTB to 50-km fiber transmission.

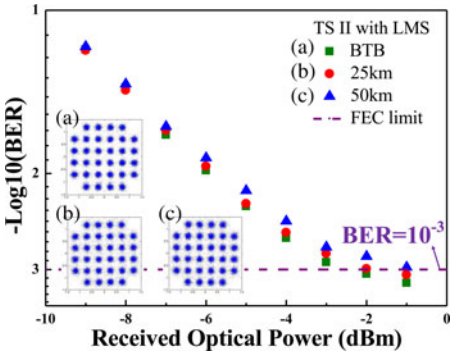

Fig. 11. BER versus received optical power curves for 6.98-GHz 32-QAM 2 × 2 MIMO OFDM signals with TS II and LMS I/Q imbalance compensation over fiber transmission from BTB to 50-km and 3.5-m wireless transmission, and the constellation diagrams. (a) At BTB transmission. (b) With 25-km fiber transmission. (c) With 50-km fiber transmission.

(a) to (d) in Fig. 10 show the constellation diagrams for BTB and 50-km transmission with 16-QAM and 32-QAM at −5 and −1 dBm received optical power, respectively. The line data rate of 55.875 and 61.875 Gb/s could be achieved with 16-QAM and 32-QAM data formats, respectively. The maximum combined spectral efficiency of two channel signals was up to 10-bit/s/Hz with the 32-QAM OFDM signal.

Fig. 11 shows the BER versus the received optical power curves of a 6.98-GHz 32-QAM OFDM signal using TS II over 3.5-m wireless transmission distance. It can be observed that there was no significant power penalty between BTB and 25-km transmission, and about 1 dB of power penalty between BTB and 50-km transmission. Insets (a)–(c) of Fig. 11 are the constellation diagrams at −1 dBm received optical power from BTB to 50-km transmission. 69.843 Gb/s line data rate was achievable with the 6.98-GHz 32-QAM OFDM signals. Due to about 10 dB variation of the frequency response as shown in Fig. 7(c), bit-loading algorithm was used to adjust power weighting factor and to optimize the data format of each subcarrier. Modulation formats, including 8-QAM, 16-QAM,

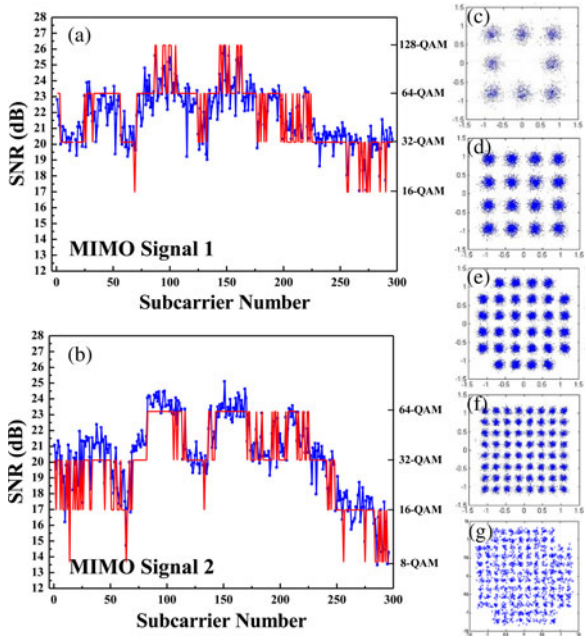

Fig. 12. SNR performance of two channels for each subcarriers of 2 × 2 MIMO OFDM signal with the TS I, LMS I/Q imbalance compensation and bit-loading algorithm over 50-km fiber transmission and 3.5-m wireless transmission. (a) MIMO signal 1, (b) MIMO signal 2, and constellation diagrams (c)–(g).

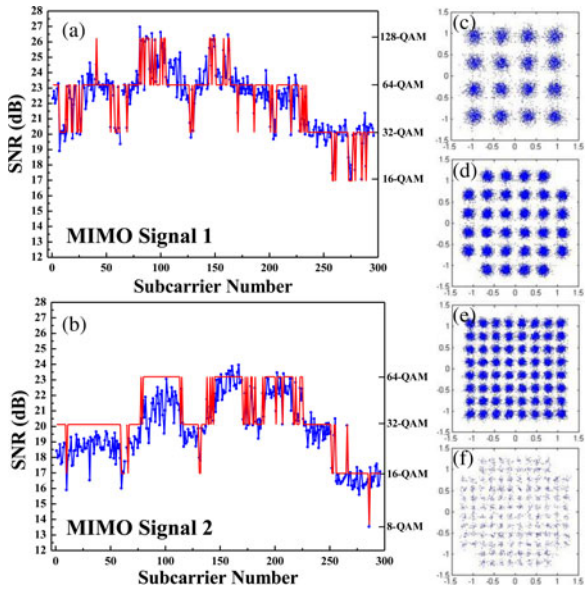

Fig. 13. SNR performance of two channels for each subcarriers of MIMO OFDM signal with TS II, LMS I/Q imbalance compensation and bit-loading algorithm over 50-km fiber transmission and 3.5-m wireless transmission. (a) MIMO signal 1, (b) MIMO signal 2, and constellation diagrams (c)–(f).

32-QAM, 64-QAM and 128-QAM, were utilized based on the corresponding SNR of each subcarrier. Fig. 12 shows the SNR and data format distribution of the 6.91-GHz wide OFDM signals with TS I. With 50-km fiber and 3.5-m wireless transmission, the data rate was increased from 55.875 to 72.797 Gb/s at –1 dBm received optical power, and the overall BER was

1×10^{-3} with LMS I/Q imbalance compensation. The corresponding constellation diagrams are shown in insets (c)–(g) in Fig. 12. For TS II, bit-loading was used to increase the data rate from 69.843 to 75.211 Gb/s as shown in Fig. 13. The corresponding constellation diagrams are also shown in the inset (c) to (f) in Fig. 13. Consequently, by applying bit-loading algorithm, the spectral efficiency of the two data streams can achieve 10.528 bit/s/Hz with TS I and 10.876 bit/s/Hz with TS II, respectively.

VI. Conclusion

We theoretically and experimentally investigated the impact of I/Q imbalance on the performance of a wideband 2×2 MIMO RoF system operating at 60 GHz. Two kinds of training symbol arrangements were considered—namely the commonly used approach and a proposed second approach, where the training symbols are split into the positive and negative subcarrier frequencies, which are in turn placed in different time-slots. Experimental results showed that the proposed training symbol arrangement performed significantly better than the commonly used approach in terms of compensating for I/Q imbalance in the transmitted 2×2 MIMO signals. It was observed that the proposed training symbol arrangement alone could achieve a similar performance to that of the commonly used training symbol approach which is combined with the Least Mean Squares (LMS) algorithm for I/Q imbalance compensation. We combined the proposed training symbol arrangement with LMS I/Q compensation and bit-loading to achieve an extremely high wireless data rate transmission of 75.211 Gb/s over both 50 km of standard single-mode fiber and 3.5 m wireless distance. Only a small optical power penalty of $\sim$1 dB was observed after 50 km fiber transmission. This result represents a high spectral efficiency of $\sim$10.876 bit/s/Hz.

References

[1] J. Capmany and D. Novak, "Microwave photonics combines two worlds," *Nat. Photon.*, vol. 1, pp. 319–330, 2007.

[2] J. Wells, "Faster than fiber: The future of multi-G/s wireless," *IEEE Microw. Mag.*, vol. 10, no. 3, pp. 104–112, May 2009.

[3] M. García Larrodé, A. M. J. Koonen, J. J. Vegas Olmos, and A. Ng'oma, "Bidirectional radio-over-fiber link employing optical frequency multiplication," *IEEE Photon. Technol. Lett.*, vol. 18, no. 1, pp. 241–243, Jan. 2006.

[4] C. T. Lin, J. Chen, P. T. Shih, W. J. Jiang, and S. Chi, "Ultra-high data-rate 60 GHz radio-over-fiber systems employing optical frequency multiplication and OFDM formats," *J. Lightw. Technol.*, vol. 28, no. 16, pp. 2296–2306, Aug. 2010.

[5] Y. T. Hsueh, Z. Jia, H. C. Chien, A. Chowdhury, J. Yu, and G. K. Chang, "Multiband 60-GHz wireless over fiber access system with high dispersion tolerance using frequency tripling technique," *J. Lightw. Technol.*, vol. 29, no. 8, pp. 1105–1111, Apr. 2011.

[6] A. Ng'oma, C. T. Lin, L.-Y. Wang He, W. J. Jiang, F. Annunziata, J. Chen, P. T. Shih, J. George, and S. Chi, "31Gbps RoF system employing adaptive bit-loading OFDM modulator at 60 GHz," presented at the Opt. Fiber Commun. Conf., Los Angeles, CA, USA, 2011, Paper OWT7.

[7] Q. Zou, A. Tarighat, and A. H. Sayed, "Compensation of phase noise in OFDM wireless systems," *IEEE Trans. Signal Process.*, vol. 55, no. 11, pp. 5407–5423, Nov. 2007.

[8] C. C. Wei, C. T. Lin, M. I Chao, and W. J. Jiang, "Adaptively modulated OFDM RoF signals at 60 GHz over long-reach 100-km transmission systems employing phase noise suppression," *IEEE Photon. Technol. Lett.*, vol. 24, no. 1, pp. 49–51, Jan. 2012.

[9] M. Weiss, A. Stohr, F. Lecoche, and B. Charbonnier, "27 Gbit/s photonic wireless 60 GHz transmission system using 16-QAM OFDM," in *Proc. Microw. Photon.*, 2009, pp. 1–3.

[10] C. L. Liu, "Impacts of I/Q imbalance on QPSK-OFDM-QAM detection," *IEEE Trans. Consum. Electron.*, vol. 44, no. 3, pp. 984–989, Aug. 1998.

[11] A. Tarighat, R. Bagheri, and A. H. Sayed, "Compensation scheme and performance analysis of IQ imbalance in OFDM receivers," *IEEE Trans. Signal Process.*, vol. 53, no. 8, pp. 3257–3268, Aug. 2005.

[12] H. S. Chung, S. H. Chang, and K. J. Kim, "Effect of IQ mismatch compensation in an optical coherent OFDM receiver," *IEEE Photon. Technol. Lett.*, vol. 22, no. 5, pp. 308–310, Mar. 2010.

[13] S. Fouladifard and H. Shafiee, "Frequency offset estimation in OFDM systems in presence of IQ imbalance," in *Proc. IEEE Commun.*, Anchorage, AK, USA, 2003, vol. 3, pp. 2071–2075.

[14] Y. Egashira, Y. Tanabe, and K. Sato, "A novel IQ imbalance compensation method with pilot-signals for OFDM system," in *Proc. Veh.r Tech. Conf.*, 2006, pp. 1–5.

[15] S. Cao, C. Yu, and P. Y. Kam, "Decision-aided joint compensation of transmitter IQ mismatch and phase noise for coherent optical OFDM," *IEEE Photon. Technol. Lett.*, vol. 24, no. 12, pp. 1066–1068, Jun. 2012.

[16] W. J. Jiang, H. Yang, Y. M. Yang, C. T. Lin, and A. Ng'oma, "40 Gb/s RoF signal transmission with 10 m wireless distance at 60 GHz," presented at the Opt. Fiber Commun. Conf., Los Angeles, CA, USA, 2012, Paper OTu2H1.

[17] E. Torkildson, U. Madhaow, and M. Rodwell, "Indoor millimeter wave MIMO: Feasibility and performance," *IEEE Trans. Wireless Comm.*, vol. 10, no. 12, pp. 4150–4160, Dec. 2011.

[18] G. L. Stuber, J. R. Barry, S. W. Mclaughlin, Y. Li, M. A. Ingram, and T. G. Pratt, "Broadband MIMO-OFDM wireless communications," *Proc. IEEE*, vol. 92, no. 2, pp. 271–294, Feb. 2004.

[19] C. T. Lin, A. Ng'oma, W.-Y. Lee, C. C. Wei, C.-Y. Wang, T.-H. Lu, J. Chen, W. Jiang, and C.-H. Ho, "2×2 MIMO radio-over-fiber system at 60 GHz employing frequency domain equalization," *Opt. Exp.*, vol. 20, no. 1, pp. 562–567, 2012.

[20] S. H. Fan, H. C. Chien, A. Chowdhury, C. Liu, W. Jian, Y. T. Hsueh, and G. K. Chang, " A novel radio-over-fiber system using the xy-MIMO wireless technique for enhanced radio spectral efficiency," presented at the 36th Eur. Conf. Exhib. Opt. Commun., Torino, Italy, 2010, Paper Th.9.B.1.

[21] S. Chen, Q. Yang, Y. Ma, and W. Shieh, "Real-time multi-gigabit receiver for coherent optical MIMO-OFDM signals," *J. Lightw. Technol.*, vol. 27, no. 16, pp. 3699–3704, Aug. 2009.

[22] J. Yu, Z. Jia, L. Yi, Y. Su, G. K. Chang, and T. Wang, "Optical millimeter wave generation or up-conversion using external modulator," *IEEE Photon. Technol. Lett.*, vol. 18, no. 1, pp. 265–267, Jan. 2006.

[23] T. Schenk, "Chapter 5 : IQ imbalance," in *RF Imperfections in High-Rate Wireless Systems*. Dordrecht, Netherlands: Springer Science, 2008.

[24] W. J. Jiang, C. T. Lin, L.-Y. Wang He, C. C. Wei, C. H. Ho, Y. M. Yang, P. T. Shih, J. Chen, and S. Chi, "32.65-Gbps OFDM RoF signal generation at 60 GHz employing an adaptive I/Q imbalance correction," presented at the 36th Eur. Conf. Exhib. Opt. Commun., Torino, Italy, 2010, Paper Th.9.B.5.

[25] I. Barhumi, G. Leus, and M. Moonen, "Optimal training design for MIMO OFDM systems in mobile wireless channels," *IEEE Trans. Signal Process.*, vol. 51, no. 6, pp. 1615–1624, Jun. 2003.

[26] Q. H. Spencer, A. L. Swindlehurst, and M. Haardt, "Zero-forcing methods for downlink spatial multiplexing in multiuser MIMO channels," in *IEEE Trans. Signal Process.*, vol. 52, no. 2, pp. 461–471, Feb. 2004.

[27] R. A. Shafik, S. Rahman, and A. H. M. Razibul Islam, "On the extended relationships among EVM, BER and SNR as performance metrics," in *Proc. Int. Conf. Electr. Comput. Eng.*, Dec. 19–21, 2006, pp. 408–411.

Chun-Hung Ho (S'11) is working toward the Ph.D. degree at the Institute of Photonic Systems, National Chiao Tung University, Tainan, Taiwan. His research interests include V/W-band radio-over-fiber systems, digital signal processing, multiple-input multiple-output techniques, and millimeter wave generation. He is a Student Member of the OSA, and the Member of the IEEE Communication Society.

Chun-Ting Lin (M'07) received the B.S. and M.S. degrees in material science and engineering from National Tsing Huang University, Hsinchu, Taiwan, in 1997 and 2001, respectively, and the Ph.D. degree in electrooptical engineering from National Chiao Tung University (NCTU), Hsinchu, Taiwan, in 2007. From 2007 to 2009, he was a Research Associate with the Department of Photonics, NCTU. In 2009, he joined the Faculty of NCTU, where he is currently an Associate Professor with the Institute of Photonic Systems. His research interests include radio-over-fiber systems, optical millimeter-/sub-terahertz-wave generation and application, optical data formats, and optoelectronic packages.

Tsung-Hung Lu received the B.S. and M.S. degrees in photonics from National Chiao Tung University, Hsinchu, Taiwan, in 2010 and 2012, respectively. His research interests include radio-over-fiber systems, digital signal processing, multiple-input multiple-output techniques, and optical millimeter wave generation.

Hou-Tzu Huang received the B.S. degree from the Department of Photonics, National Chiao Tung University, Hsinchu, Taiwan, in 2011. He is currently working toward the Ph.D. degree at the Institute of Photonics System, National Chiao Tung University. His current research interests include radio-over-fiber systems, fiber/wireless MIMO technique and digital signal processing.

Boris (Po-Tsung) Shih received the M.S. degree from the Department of Electrophysics and the Ph.D. degree from the Department of Photonics, National Chiao Tung University, Hsinchu, Taiwan, in 2006 and 2010, respectively. In 2011, he joined Corning Inc., Hsinchu, Taiwan, as a Scientist, where he is currently working in the Research Center. He has been working on the research projects in fiber-wireless technologies, optical communication system, and communication signal processing.

Chia-Chien Wei received the Ph.D. degree in electro-optical engineering from National Chiao Tung University, Hsinchu, Taiwan, and the Ph.D. degree in electrical engineering from the University of Maryland, Baltimore County, MD, USA, in 2008. In 2011, he joined National Sun Yat-Sen University, Kaohsiung, Taiwan, where he is currently an Assistant Professor at the Department of Photonics. His current research interests include optical and electrical signal processing, advanced modulation formats, optical access networks, and radio-over-fiber systems.

Anthony Ng'oma (M'02) received the M.Eng. and B.Eng. degrees (with merit) in electrical/electronics engineering from the University of Zambia, Lusaka, Zambia. He received the Ph.D. degree in optical fiber communications and the PD.Eng. degree in information and communication technology, both from the Eindhoven University of Technology, Eindhoven, The Netherlands. He leads a team of scientists and engineers working on short-reach communication networks and applications at the main research center for Corning Inc., Corning, NY, USA. He has been actively involved in optical communications research in general and fiber-wireless technology research in particular, for more than ten years, both in Europe and the United States. He has authored and coauthored more than 60 peer-reviewed technical publications and journals and two book chapters in the field of fiber-optic communication. He is a Member of the IEEE Photonics Society and the IEEE Microwave Theory and Techniques Society.